CNN-Based Segmentation of the Cardiac Chambers and Great Vessels in Non-Contrast-Enhanced Cardiac CT

Steffen Bruns[1] S.BRUNS@UMCUTRECHT.NL
Jelmer M. Wolterink[1] J.M.WOLTERINK@UMCUTRECHT.NL
Robbert W. van Hamersvelt[2] R.W.VANHAMERSVELT-3@UMCUTRECHT.NL
Tim Leiner[2] T.LEINER@UMCUTRECHT.NL
Ivana Išgum[1] I.ISGUM@UMCUTRECHT.NL
[1] *Image Sciences Institute, UMC Utrecht, Heidelberglaan 100, 3584CX Utrecht, the Netherlands*
[2] *Department of Radiology, UMC Utrecht, Heidelberglaan 100, 3584CX Utrecht, the Netherlands*

Editors: Under Review for MIDL 2019

Abstract

Quantification of cardiac structures in non-contrast CT (NCCT) could improve cardiovascular risk stratification. However, setting a manual reference to train a fully convolutional network (FCN) for automatic segmentation of NCCT images is hardly feasible, and an FCN trained on coronary CT angiography (CCTA) images would not generalize to NCCT. Therefore, we propose to train an FCN with virtual non-contrast (VNC) images from a dual-layer detector CT scanner and a reference standard obtained on perfectly aligned CCTA images.

1. Introduction

Patients at risk of cardiovascular disease (CVD) may be identified based on accurate volumetric quantification of the cardiac structures (Nagarajarao et al., 2008; Narayanan et al., 2014). Such quantification is feasible in coronary CT angiography (CCTA) (Raman et al., 2006) and several automatic methods have been proposed to segment cardiac structures in CCTA (Ecabert et al., 2008; Zheng et al., 2008; Kirişli et al., 2010; Zhuang et al., 2019).

However, many patients only undergo non-contrast CT (NCCT) scanning (Sandfort and Bluemke, 2017). It would thus be valuable to determine volumes of cardiac structures from the NCCT scan of these patients. Unfortunately, methods developed for segmentation in CCTA do not generalize to the NCCT domain. Recently, Shahzad et al. (2017) have shown that segmentations of cardiac structures in the CCTA domain can be translated to the NCCT domain through multi-atlas segmentation. However, this approach requires a challenging inter-modality registration between CCTA and NCCT images.

To address this, we propose to train a fully convolutional network (FCN) for the segmentation of cardiac structures in NCCT using virtual-non-contrast (VNC) images (Figure 1). VNC images mimic real NCCT images, but are reconstructed from a CT acquisition *with* contrast-enhancement using a dual-layer detector CT scanner. Hence, a VNC image is perfectly aligned with the CCTA image of the same acquisition, and reference segmentations obtained in CCTA images can directly be used in the corresponding VNC images.

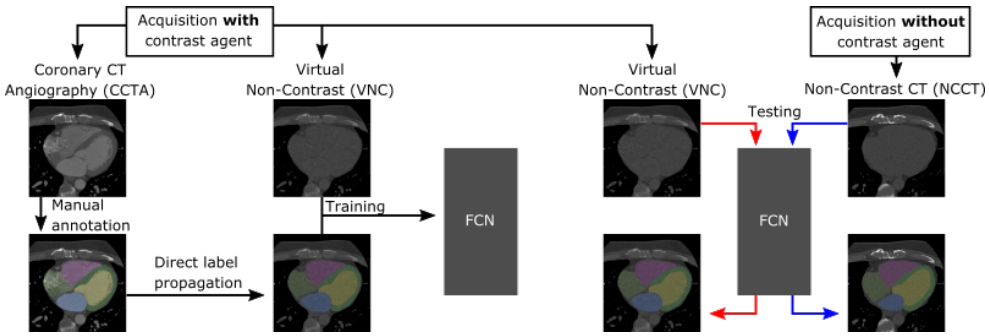

Figure 1: Method overview. Left: A fully convolutional network (FCN) is trained with VNC images and CCTA segmentations. CCTA and VNC images are made in a single acquisition and thus, their segmentations are perfectly aligned. Right: The FCN automatically segments cardiac structures in both VNC and NCCT images.

2. Materials and methods

We used a primary data set (van Hamersvelt et al., 2019) consisting of CT images of 18 patients scanned on a Philips IQon dual-layer-detector CT scanner (Philips Healthcare, Best, The Netherlands). Hence, a CT acquisition with contrast enhancement could be reconstructed into a CCTA and a VNC image and these two images were perfectly aligned. Thus, reference segmentations of seven cardiac structures (left ventricular [LV] cavity, right ventricle, left atrium, right atrium, LV myocardium, ascending aorta, pulmonary artery trunk) obtained on CCTA images delineated the same structures on the VNC images. We also included a secondary data set consisting of 218 NCCT images with corresponding CCTA images to evaluate the capability of our method to segment NCCT images. These images were acquired on a Philips Brilliance iCT scanner (Philips Healthcare, Best, The Netherlands) without the option to reconstruct VNC images. All images had 0.34–0.56 mm^2 in-plane resolution, and 0.9 mm and 0.45 mm slice thickness and increment, respectively.

The FCN architecture we used is based on the 2D residual FCN proposed by Johnson et al. (2016). We adapted the network to operate on 256×256×5 voxel 3D inputs and output 256×256×1 voxel predictions. We set the number of downsampling and upsampling layers to three, and the number of residual blocks to six. The FCN was trained with a mini-batch size of 32. Prior to training or testing, images were smoothed with a moderate Gaussian filter and resampled to an isotropic resolution of $0.8 \times 0.8 \times 0.8$ mm^3. A connected component labeling was performed on obtained segmentations and for each structure, the largest connected component was retained in the final segmentation result.

The automatic segmentations on VNC images from the primary data set were evaluated quantitatively using the Dice similarity coefficient (DSC) and the average symmetric surface distance (ASSD). In the secondary data set, an expert inspected each NCCT image, the automatic NCCT segmentation, and the corresponding CCTA image, and assigned a grade to the segmentation based on the criteria proposed by Abadi et al. (2010) where *Grade 1* corresponds to very accurate segmentations and *Grade 5* to a failed segmentation.

Table 1: Average (± SD) per-class Dice similarity coefficients (DSC) and average symmetric surface distances (ASSD, in mm) between reference segmentations and automatic segmentations on virtual non-contrast (VNC) images for left ventricular cavity (LV-C) and myocardium (LV-M), right ventricle (RV), left atrium (LA), right atrium (RA), ascending aorta (AA), and pulmonary artery (PA) trunk.

	LV-C	**LV-M**	**RV**	**LA**	**RA**	**AA**	**PA**
DSC	0.89 ± 0.03	0.84 ± 0.04	0.91 ± 0.03	0.92 ± 0.01	0.90 ± 0.04	0.94 ± 0.01	0.86 ± 0.06
ASSD	1.67 ± 0.49	1.15 ± 0.27	1.38 ± 0.56	1.19 ± 0.35	1.48 ± 0.61	0.75 ± 0.24	1.97 ± 1.55

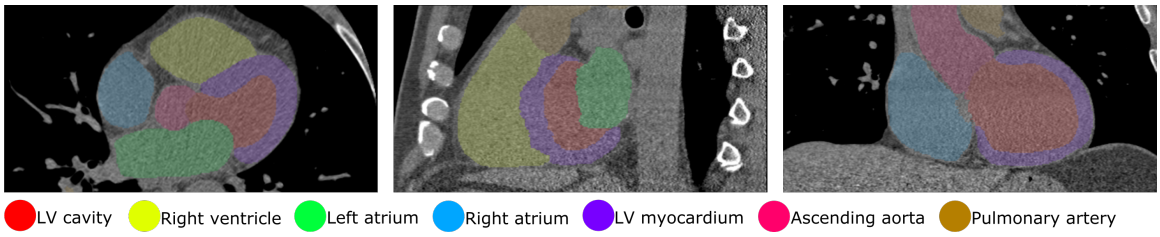

Figure 2: Automatic segmentation in a non-contrast CT image (secondary data set).

3. Experiments and results

We performed a six-fold nested cross-validation on the 18 VNC images from the primary data set. An ensemble of six models, one for each cross-validation fold, was used for testing on the secondary data set. Each model was trained for 10000 iterations using Adam optimization, an initial learning rate of 0.001, and a 70% learning rate decay every 2000 iterations. The negative sum of soft Dice scores over all classes was used as the loss function.

Table 1 lists quantitative results for the automatic segmentations in the 18 VNC images from the primary data set. Automatic segmentations of the 218 NCCT images in the secondary data set were qualitatively evaluated to assess the generalization of trained models to NCCT images. The expert assigned 27 segmentations (12%) to Grade 1 (very accurate), 119 segmentations (55%) to Grade 2, 42 segmentations (19%) to Grade 3, 15 segmentations (7%) to Grade 4, and 15 segmentations (7%) to Grade 5 (segmentation failed). Hence, most segmentations contained slight errors that are unlikely to significantly impact volume measurements. Figure 2 shows an automatic segmentation on an NCCT image.

4. Discussion and conclusion

We have presented an FCN that is able to segment seven cardiac structures in both VNC images and NCCT images. This allows accurate volume quantification of the cardiac chambers and great vessels even in the absence of contrast medium injection. Here, we addressed domain adaptation by using the physics properties of the dual-layer detector CT scanner, but future work may employ adversarial domain adaptation to translate images from the VNC domain to the NCCT domain (Lafarge et al., 2017).

Acknowledgments

This research is supported by the Dutch Technology Foundation STW, which is part of the Netherlands Organisation for Scientific Research (NWO) and partly funded by the Ministry of Economic Affairs and Philips Healthcare. We gratefully acknowledge the support of NVIDIA Corporation with the donation of the Titan Xp GPU used for this research.

References

Sobhi Abadi, Ariel Roguin, Ahuva Engel, and Jonathan Lessick. Feasibility of automatic assessment of four-chamber cardiac function with MDCT: initial clinical application and validation. *European Journal of Radiology*, 74(1):175–181, 2010.

Olivier Ecabert, Jochen Peters, Hauke Schramm, Cristian Lorenz, Jens von Berg, Matthew J Walker, Mani Vembar, Mark E Olszewski, Krishna Subramanyan, Guy Lavi, et al. Automatic model-based segmentation of the heart in CT images. *IEEE Transactions on Medical Imaging*, 27(9):1189, 2008.

Justin Johnson, Alexandre Alahi, and Li Fei-Fei. Perceptual losses for real-time style transfer and super-resolution. In *European Conference on Computer Vision*, pages 694–711. Springer, 2016.

Hortense A Kirişli, Michiel Schaap, Stefan Klein, Stella-Lida Papadopoulou, Mara Bonardi, Chin-Hui Chen, Annick C Weustink, Nico R Mollet, Evert-Jan Vonken, Rob J van der Geest, et al. Evaluation of a multi-atlas based method for segmentation of cardiac CTA data: a large-scale, multicenter, and multivendor study. *Medical Physics*, 37(12):6279–6291, 2010.

Maxime W Lafarge, Josien PW Pluim, Koen AJ Eppenhof, Pim Moeskops, and Mitko Veta. Domain-adversarial neural networks to address the appearance variability of histopathology images. In *Deep Learning in Medical Image Analysis and Multimodal Learning for Clinical Decision Support*, pages 83–91. Springer, 2017.

Harsha S Nagarajarao, Alan D Penman, Herman A Taylor, Thomas H Mosley, Kenneth Butler, Thomas N Skelton, Tandaw E Samdarshi, Giorgio Aru, and Ervin R Fox. The predictive value of left atrial size for incident ischemic stroke and all-cause mortality in African Americans: the atherosclerosis risk in communities (ARIC) study. *Stroke*, 39(10): 2701–2706, 2008.

Kumar Narayanan, Kyndaron Reinier, Carmen Teodorescu, Audrey Uy-Evanado, Ryan Aleong, Harpriya Chugh, Gregory A Nichols, Karen Gunson, Barry London, Jonathan Jui, et al. Left ventricular diameter and risk stratification for sudden cardiac death. *Journal of the American Heart Association*, 3(5):e001193, 2014.

Subha V Raman, Mona Shah, Beth McCarthy, Anne Garcia, and Amy K Ferketich. Multi–detector row cardiac computed tomography accurately quantifies right and left ventricular size and function compared with cardiac magnetic resonance. *American Heart Journal*, 151(3):736–744, 2006.

Veit Sandfort and David A Bluemke. CT calcium scoring. History, current status and outlook. *Diagnostic and Interventional Imaging*, 98(1):3–10, 2017.

Rahil Shahzad, Daniel Bos, Ricardo PJ Budde, Karlijn Pellikaan, Wiro J Niessen, Aad van der Lugt, and Theo van Walsum. Automatic segmentation and quantification of the cardiac structures from non-contrast-enhanced cardiac CT scans. *Physics in Medicine & Biology*, 62(9):3798, 2017.

Robbert W van Hamersvelt, Ivana Išgum, Pim A de Jong, Maarten JM Cramer, Geert EH Leenders, Martin J Willemink, Michiel Voskuil, and Tim Leiner. Application of speCtraL computed tomograAphy to impRove specIficity of cardiac compuTed tomographY (clarity study): rationale and design. *BMJ Open*, 9(3):e025793, 2019.

Yefeng Zheng, Adrian Barbu, Bogdan Georgescu, Michael Scheuering, and Dorin Comaniciu. Four-chamber heart modeling and automatic segmentation for 3-D cardiac CT volumes using marginal space learning and steerable features. *IEEE Transactions on Medical Imaging*, 27(11):1668–1681, 2008.

Xiahai Zhuang, Lei Li, Christian Payer, Darko Stern, Martin Urschler, Mattias P Heinrich, Julien Oster, Chunliang Wang, Orjan Smedby, Cheng Bian, Xin Yan, Pheng-Ann Heng, Aliasghar Mortazi, Ulas Bagci, Guanyu Yang, Chenchen Sun, Gaetan Galisot, Jean-Yves Ramel, Thierry Brouard, Qianqian Tong, Weixin Si, Xiangyun Liao, Guodong Zeng, Zenglin Shi, Guoyan Zheng, Chengjia Wang, Tom MacGillivray, David Newby, Kawal Rhode, Sebastien Ourselin, Raad Mohiaddin, Jennifer Keegan, David Firmin, and Yang Guang. Evaluation of algorithms for multi-modality whole heart segmentation: An open-access grand challenge. *arXiv preprint*, https://arxiv.org/abs/1902.07880, 2019.